MINERALOGY OF THE MARTIAN MANTLE INFERRED FROM BULK CHEMICAL COMPOSITIONS OF MARS. S. Yang[1], M. Humayun[1], K. Righter[2], A. J. Irving[3], R. H. Hewins[4,5] and B. Zanda[4,6]. [1]Florida State University, Tallahassee, FL 32310, USA (syang@magnet.fsu.edu); [2]NASA Johnson Space Center, Mail code XI2, Houston, TX 77058, USA; [3]Department of Earth and Space Sciences, University of Washington, Seattle, WA 98195, USA; [4]IMPMC, Sorbonne Université, MNHN-UPMC, 75005 Paris, France; [5]Rutgers University, Piscataway, NJ 08854, USA; [6]IMCCE, Observatoire de Paris - CNRS UMR 8028, 75014 Paris, France.

Introduction: The mineralogical composition of a planet's mantle determines the composition of the volcanism that plays an important role in the composition of the surface environment: crust, atmosphere and hydrosphere or biosphere. On Earth, mantle xenoliths and peridotite outcrops provide essential clues to the mineralogical composition of the mantle [1]. The mineralogical composition of Mars' mantle is not known from direct samples. In this study, the mineralogy of the martian mantle is constrained by using the MELTS code [2-3] to model the solidus mineralogy of published estimates of the bulk composition of the martian mantle. Phase compositions from experimental studies of the melting of putative martian mantle compositions [4-6] are used to validate the MELTS output.

Method: We used the AlphaMELTS front end for the algorithm and the pMELTS calibration [2] to calculate solidus phase relations of martian mantle. Eight compositional models of bulk silicate Mars [7-14] were taken as the starting compositions to perform the MELTS calculation of phase equilibria in the solidus. The sources of model compositions of Mars are named using author initials and year of publication. Two experimental starting compositions resembling WD94 [9] used in experimental studies [5, 15] were also modeled for validation purposes. The pMELTS calculations were performed at pressures of 2, 3, 4 and 5 GPa to constrain the mantle mineralogy of the sources of shergottites. At each pressure, mineralogies were calculated at the solidus temperature. The initial Fe^{2+}/Fe^{3+} ratio was set to 3 log units beneath the quartz-fayalite-magnetite (QFM-3) buffer [16], and the calculation was ran unbuffered [17]. No water was assumed in our MELTS calculations.

Results: MELTS calculations agree well with experimental data within the pressure interval 2-4 GPa for olivine, cpx and garnet (± 1 wt.%) (Fig. 1). The mismatch in opx (3 wt.%) between MELTS calculations and experimental data (Fig. 1) is due to a known limitation: MELTS over-estimates the stability of orthopyroxene relative to olivine [18]. At pressures of 5 GPa and above, the MELTS calculation deviates increasingly from the experimental data (Fig. 1), as the pMELTS algorithm is outside of its calibrated pressure range [17]. As shown in Fig. 1, the effect of pressure on the solidus mineral mode between 2-4 GPa is minor. Varying temperature by 100 °C below the solidus only causes 1 wt.% variations in opx and cpx modes; and shows no effect on the modes of olivine and garnet (not shown).

MELTS failed to converge to a solution for the starting composition of KC08 [12] because of the absence of TiO_2 data. The solidus mineral assemblages calculated by MELTS for nine modeled martian compositions (MA79, OK92, WD94, LF97, S99, AD04, T13, M13 and YM20) [5, 7-11, 13-15] at 3 GPa are shown in Fig. 2, with the martian mantle mineralogy at 3 GPa provided in YM20 [14] and two literature mineralogy modes (BD03 and D08) [19-20] for comparison. The mineral modes of YM20 composition constrained using MELTS are comparable to that calculated using Perple_X in [14]. All compositions yielded mineral assemblages consisting of olivine, cpx, opx and garnet, except opx is absent from the mineral assemblages of MA79 [7], and garnet barely exists in the mineral assemblages of LF97 [10] and S99 [11] compositions (Fig. 2).

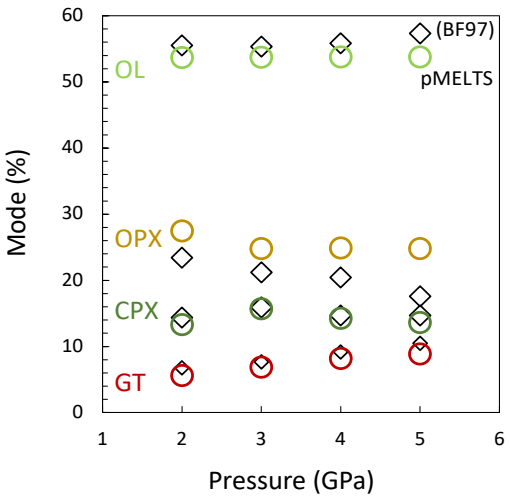

Fig. 1: The solidus mineralogy of the WD94 composition against pressure calculated by MELTS compared with experimental solidus mode [4] .

In Fig. 3, solidus modes of each mineral phase (olivine, cpx, opx and garnet) at 3 GPa are plotted against a series of elemental ratios (Mg/Si, Ca/Si and Al/Si) of bulk model compositions of Mars. Three experimental runs (BF-39, OD940 and G312) at 3 GPa [4-6] are also shown for comparison. As expected, olivine modes correlate with bulk Mg/Si ratios (Fig. 3a), opx modes anticorrelate with bulk Ca/Si ratios (Fig. 3b), whereas cpx modes correlate with bulk Ca/Si ratios (Fig. 3c), and

garnet modes correlate with bulk Al/Si ratios (Fig. 3d). But cpx yielded by high-Na_2O bulk compositions (S99 and LF97) [10,11] are too high to follow the cpx-Ca/Si correlations (Fig. 3c) due to the presence of excess jadeite component in the pyroxene.

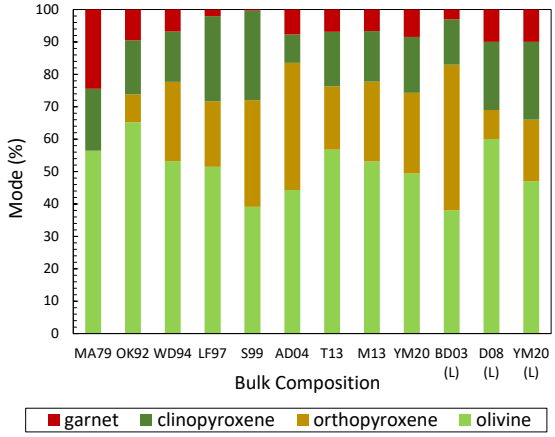

Fig. 2: The solidus mineral assemblages calculated by MELTS for nine modeled martian compositions.

Discussion: Despite the overestimation of the stability of opx over olivine (Fig. 1), the calculation of solidus mineral assemblages using the MELTS algorithm is in good agreement with the experimentally determined mineralogy [4-6] of martian mantle. The MELTS-based approach yielded a similar mineralogy to that of [14], indicating that the mineral abundances obtained are not sensitive to the choice of software used.

More importantly, a series of MELTS calculations performed in this study allowed us to examine the effect of composition on the mantle mineralogy of Mars (Fig. 3). For example, MgO content of OK92 [8] is known to be overestimated [13], so that the 65 wt.% olivine yielded by this composition is too high to be realistic. A synthetic composition from AD04 [15] produced the highest opx (~ 40%) (Fig. 2) because it is depleted in CaO. Compositions LF97 [10] and S99 [11] overestimated volatile contents such as Na_2O [13], and thus produced ~ 20 % jadeite in cpx phases (Fig. 3c). But the jadeite-corrected cpx modes of S99 and L97 are still higher than cpx modes of other compositions (Fig. 3c). The composition MA79 overestimated Al_2O_3 [13] and thus produced over 20 wt. % garnet. Two compositions (LF97 and S99) [10,11] with low Al_2O_3/SiO_2 produced very little (~ 2%) or no garnet (Fig. 2).

In this study, we adopted each model composition of Mars as an individual starting composition, assuming a homogeneous, undifferentiated bulk silicate Mars (BSM). A small degree of partial melting (~ 4 %) of BSM is needed to extract the primary martian crust [21]. Experimental melting of martian compositions have shown that the changes in mineralogy caused by 4 % melting is negligible [5-6]. Thus, in a companion study [22], the MELTS modeled mineralogy of BSM compositions [7-16] from this study, together with the experimentally determined partition coefficients (D_i) between minerals and melts [e.g., 23, 24], were used to constrain the bulk partition coefficients of trace elements (D_E) in the shergottite source.

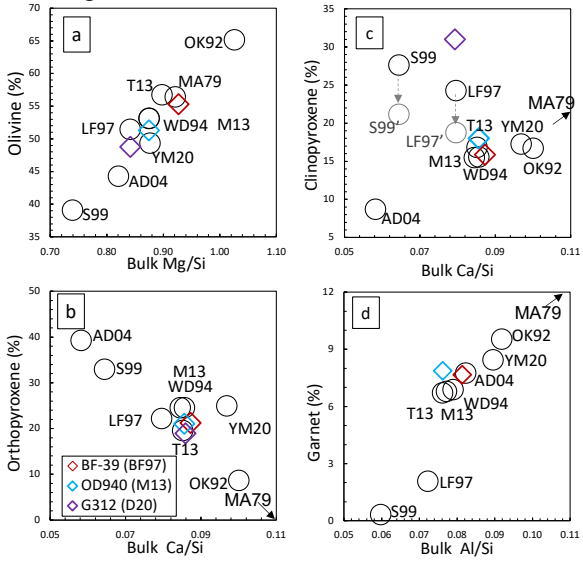

Fig. 3: The correlations of solidus modes against bulk elemental ratios of starting compositions.

References: [1] Jagoutz E. et al. (1979) In *LPSC Proceedings 10,* 2031-2050. [2] Ghiorso M. S., & Sack, R. O. (1995) *Contrib. to Mineral. Petrol. 119,* 197-212. [3] simow P. D., & Ghiorso M. S. (1998) *Am. Mineral. 83*,1127-1132. [4] Bertka C. M., & Fei, Y. (1997) *JGR: Solid Earth 102,* 5251-5264. [5] Matsukage K. N. et al. (2013) *J. Mineral. Petrol. Sci.* 120820. [6] Ding, S. et al. (2020). JGR*: Planets 125,* e2019JE006078. [7] Morgan J. W., & Anders E. (1979) *GCA 43,* 1601-1610. [8] Ohtani E., & Kamaya N. (1992) *GRL 19,* 2239-2242. [9] Wänke H., & Dreibus G. (1994) *Series A: Phys. Eng. Sci. 349.1690,* 285-293. [10] Lodders K., & Fegley Jr, B. (1997) *Icarus 126,* 373-394. [11] Sanloup C. et al. (1999) *Phys. Earth Planet. Inter. 112,* 43-54. [12] Khan A., & Connolly J. A. D. (2008). *JGR: Planets, 113*(E7). [13] Taylor G. J. (2013) *Geochemistry 73,* 401-420. [14] Yoshizaki T., & McDonough W. F. (2020) *GCA 273,* 137-162. [15] Agee C. B., & Draper D. S. (2004) *EPSL 224,* 415-429. [16] Herd C. D. (2008) *Rev. Mineral. Geochem. 68*, 527-553. [17] Balta J. B., & McSween Jr H. Y. (2013) JGR*: Planets 118*, 2502-2519. [18] Hirschmann M. M. et al. (1998) *GCA 62*, 883-902. [19] Borg L. & Draper D. S. (2003) *MaPS 38,* 1713-1731. [20] Debaille V. et al. (2008) *EPSL* 269, 186-199. [21] Humayun M. et al. (2013) *Nature 503.7477,* 513-516. [22] Yang S. et al. (2022b) LPSC LIII abstract (submitted). [23] Blinova A. and Herd C. (2009) *GCA 73,* 3471-3492. [24] Salters V.J. et al. (2002) *G³ 3,* 1-23.